J Physiol 591.23 (2013) pp 5879–5893

The Journal of Physiology

A single point mutation reveals gating of the human ClC-5 Cl^-/H^+ antiporter

Silvia De Stefano, Michael Pusch and Giovanni Zifarelli

Istituto di Biofisica, CNR, Via De Marini 6, I-16149 Genova, Italy

Key points

- ClC-5 is a $2Cl^-/1H^+$ antiporter expressed in endosomes that is essential for proper endocytosis, but its molecular function is still not understood.
- In heterologous systems ClC-5 elicits currents only at positive potentials. This rectifying behaviour conflicts with most of the models proposed to explain ClC-5 function. The origin of this rectification is unknown.
- Here we identified a ClC-5 mutation, D76H, that elicits inward tail currents at negative potentials.
- These currents reflect transmembrane transport that preserve the $2Cl^-/1H^+$ stoichiometry.
- We conclude that a gating mechanism regulates ClC-5 transport activity and is at least in part responsible for the strong rectification of ClC-5 currents.

Abstract ClC-5 is a $2Cl^-/1H^+$ antiporter highly expressed in endosomes of proximal tubule cells. It is essential for endocytosis and mutations in ClC-5 cause Dent's disease, potentially leading to renal failure. However, the physiological role of ClC-5 is still unclear. One of the main issues is whether the strong rectification of ClC-5 currents observed in heterologous systems, with currents elicited only at positive voltages, is preserved *in vivo* and what is the origin of this rectification. In this work we identified a ClC-5 mutation, D76H, which, besides the typical outward currents of the wild-type (WT), shows inward tail currents at negative potentials that allow the estimation of the reversal of ClC-5 currents for the first time. A detailed analysis of the dependence of these inward tail currents on internal and external pH and $[Cl^-]$ shows that they are generated by a coupled transport of Cl^- and H^+ with a 2 : 1 stoichiometry. From this result we conclude that the inward tail currents are caused by a gating mechanism that regulates ClC-5 transport activity and not by a major alteration of the transport mechanism itself. This implies that the strong rectification of the currents of WT ClC-5 is at least in part caused by a gating mechanism that activates the transporter at positive potentials. These results elucidate the biophysical properties of ClC-5 and contribute to the understanding of its physiological role.

(Received 11 June 2013; accepted after revision 30 September 2013; first published online 7 October 2013)
Corresponding author G. Zifarelli: Istituto di Biofisica, CNR, Via De Marini 6, I-16149 Genova, Italy. Email: zifarelli@ge.ibf.cnr.it

Abbreviations NMDG, *N*-methyl-D-glucamine; WT, wild type.

Introduction

CLC proteins comprise both Cl^- channels and Cl^-/H^+ antiporters found in all phyla (Jentsch, 2008). In humans they control several physiological functions, such as muscle excitability, transepithelial transport, endocytosis, lysosomal function and synaptic activity (Zifarelli & Pusch, 2007; Stauber *et al.* 2012). Interestingly, this family breaks an established biophysical paradigm according to which passive diffusion mediated by ion channels and coupled, thermodynamically uphill substrate movement mediated by transporters require an intrinsically different

DOI: 10.1113/jphysiol.2013.260240

protein architecture (Accardi & Miller, 2004). In fact, structural and functional evidence suggests that CLC channels and transporters share a very similar structure (Dutzler *et al.* 2002, 2003; Estévez *et al.* 2003; Lin & Chen, 2003; Engh & Maduke, 2005).

The crystal structures of the bacterial and eukaryotic homologues ClC-ec1 (Dutzler *et al.* 2002, 2003) and ClC-Cm (Feng *et al.* 2010) show that the protein assembles as a homodimer with two subunits harbouring a narrow permeation pathway (Fig. 1*A*) containing three anion binding sites defined, from the extracellular to the intracellular side, as S_{ext}, S_{cen} and S_{in} (Fig. 1). These structures also explain the critical role of a conserved glutamate residue for the gating of CLC proteins; indeed, it is also called 'gating glutamate' (E148 in ClC-ec1 and E211 in ClC-5). In the structure of wild type (WT) ClC-ec1 represented in Fig. 1*B* and *C*, the side chain of E148 occupies S_{ext} and isolates the anion at S_{cen} from the extracellular space (Dutzler *et al.* 2002). In the structure of the E148Q mutant, an anion occupies S_{ext}, whereas the glutamine side chain is displaced from the pore (Dutzler *et al.* 2003). Recently, the structure of ClC-Cm revealed that the glutamate side chain can also be oriented towards the intracellular side and occupy S_{cen} (Feng *et al.* 2010). These structural data rationalize functional evidence showing that mutations of the gating glutamate abrogate gating in CLC channels (Fahlke *et al.* 1997; Dutzler *et al.* 2003; Traverso *et al.* 2003) and render the transporters ClC-5 and ClC-ec1 passive Cl^- conductances (Friedrich *et al.* 1999; Accardi *et al.* 2004). Another critical residue for CLC transporters is an off-pore glutamate (E203 in ClC-ec1, E268 in ClC-5), also called 'proton glutamate' (Fig. 1*B*), because it serves probably as the internal proton acceptor. Mutation of the proton glutamate to glutamine in ClC-ec1 abolishes H^+ transport and renders the transporter a passive Cl^- conductance, similar to mutations of the gating glutamate (Accardi *et al.* 2005). In ClC-5, neutralization of the corresponding residue (for example with the mutation E268A) has a different effect; it inhibits steady-state transport (Zdebik *et al.* 2008), but the mutant exhibits large transient currents upon positive voltage steps (Smith & Lippiat, 2010), which most likely originate from partial steps in the reaction cycle (Zifarelli *et al.* 2012).

ClC-5 is a $2Cl^-/1H^+$ antiporter (Zifarelli & Pusch, 2009), mostly expressed in proximal tubule cells of the kidney, where it co-localizes with the vacuolar-type H^+-ATPase in endosomal membranes (Günther *et al.* 1998) and is essential for proper endocytic function (Stauber & Jentsch, 2013). Indeed, mutations in ClC-5 lead to Dent's disease, a genetic disease caused by impaired endocytosis, characterized by hypercalciuria, nephrocalcinosis, kidney stones and renal failure (Lloyd *et al.* 1996). Studies with knock-out mice showed that ClC-5 is essential for proper endocytic activity (Piwon *et al.* 2000; Wang *et al.* 2000; Günther *et al.* 2003). Moreover, studies with knock-in mice carrying uncoupling mutations demonstrated that the Cl^-/H^+ antiport activity is physiologically relevant and cannot be substituted by a passive Cl^- conductance as previously hypothesized (Novarino *et al.* 2010). However, the physiological role of ClC-5 *in vivo* is still poorly understood (Stauber & Jentsch, 2013).

Plasma membrane expression of cloned ClC-5 in both mammalian cells and *Xenopus* oocytes gives rise to extremely outwardly rectifying currents (Steinmeyer *et al.* 1995; Friedrich *et al.* 1999) that are active only at positive potentials (cytoplasmic potential positive with respect to the extracellular potential), producing Cl^- transport only from the extracellular space into the cytoplasm and H^+ movement only out of the cell. This orientation of ion fluxes, if conserved when ClC-5 is expressed in endosomes, poses a serious challenge for the interpretation of its physiological role (Lippiat & Smith, 2012). The study of Novarino *et al.* (2010) suggested that endosomal Cl^- accumulation (equivalent to Cl^- movement towards the extracellular space) by ClC-5 could be critical for proper endocytic activity, but this direction of Cl^- movement is not observed at the plasma membrane. Moreover, the difference in the electrochemical potential between cytoplasm and endosome interior is expected to be negative and therefore unable to activate ClC-5 (Lippiat & Smith, 2012). However, theoretical calculations based on a simplified model of intracellular vesicles have suggested that, in the presence of ClC-5, the electrochemical potential difference might become positive and ClC-5 could mediate endosomal Cl^- accumulation (Weinert *et al.* 2010). However, this hypothesis has not been confirmed experimentally, and other authors emphasize the role of CLCs as mediators of Cl^- counterion movement in endosomal/lysosomal conductances (Ishida *et al.* 2013). These problems clearly highlight the need for a deeper understanding of the origin of ClC-5 rectification, i.e. the mechanism determining the direction of ion flux. In particular, it is important to understand whether ClC-5 rectification is caused by a gating mechanism or by intrinsic properties of the transport cycle.

The concept of gating is well established for ion channels, but relatively uncommon and unexplored for transporters (Hilgemann, 1996). For ion channels, the gate controls the opening/closing of the permeation pore. By analogy, for transporters, the concept of gating would indicate a mechanism that controls whether the transporter is in an active, transport-competent state, or is inactive (Fig. 10). For CLC channels it is well known that the gating processes are complex and heavily dependent on the permeant anion and on pH (Zifarelli & Pusch, 2010), and any gating processes of CLC transporters can be expected to be similarly complex. Several groups have previously suggested the existence of a gating mechanism

for CLC transporters (Zdebik *et al.* 2008; Alekov & Fahlke, 2009). However, the evidence is relatively indirect, relying on the interpretation of noise spectra (Zdebik *et al.* 2008) or mostly based on the behaviour of the transporters in the presence of uncoupling anions that deeply alter the normal transport mechanism (Alekov & Fahlke, 2009). Indeed, under uncoupling conditions, the transport cycle of CLC antiporters is stalled in a specific conformation that allows substrate permeation only according to its electrochemical gradient, similar to ion channels (Nguitragool & Miller, 2006). The clearest evidence for CLC transporter gating was recently obtained for ClC-7/Ostm1 (Leisle *et al.* 2011). The transporter activates with slow kinetics (time scale on the order of seconds) at positive voltages and deactivates also rather slowly at negative voltages. In contrast, for ClC-5, the response to a positive voltage step is dominated by a quasi-instantaneous component (Zdebik *et al.* 2008), and no inward tail currents are resolvable at negative voltages (Zifarelli & Pusch, 2009). Thus, if a gating process is present in ClC-5, it is considerably faster than for ClC-7. Moreover, ClC-5 and ClC-7 are not only different in terms of current kinetics. ClC-7 belongs to a different branch of the CLC protein family with a number of additional properties that differentiate it from ClC-5 (lysosomal expression, necessity of the beta subunit Ostm1 and neutralization of lysosomal sorting motifs for functional expression at the plasma membrane, different anion selectivity) (Leisle *et al.* 2011). Therefore, even if the mechanism of coupled Cl^-/H^+ transport appears to be conserved, the presence of a gating mechanism regulating the transport activity of ClC-7/Ostm1 does not *per se* imply that the same mechanism is present in ClC-5.

In order to uncover possible gating relaxations related to transport activity in ClC-5, we mutated a conserved aspartate residue (Fig. 1 and Fig. S1). In contrast with WT ClC-5, the mutant D76H has a slower activation at positive voltages and displays inward tail currents at negative voltages that represent movement of Cl^- and H^+ in the opposite direction compared with that which has been observed so far for WT. We performed a detailed investigation of the dependence of the inward tail currents on the internal and external proton and Cl^- concentration and temperature. We conclude that the inward tail currents reflect the relaxation of a gating process in ClC-5 that contributes to its rectifying behaviour. Moreover, we characterized, for the first time, the dependence of this gating of transport currents on voltage, pH and temperature.

Methods

Ethical approval

Oocyte harvesting from *Xenopus laevis* frogs was performed according to the Italian Government Legislation on the ethical treatment of animals. After surgery, frogs were allowed to recover from anaesthesia and suitable aftercare was given. Frogs were used two or three times for oocyte harvesting, allowing for at least 2 months of recovery between the operations. After the final operation, frogs were deeply anesthetized and then killed by decapitation in agreement with the standards of *The Journal of Physiology* (Drummond 2009: http://jp.physoc.org/content/587/4/713.full.pdf± html). The anaesthetic used was tricaine (ethyl 3-aminobenzoate methanesulfonate salt, Sigma, St Louis, MO, USA) at a concentration of $1.5\,g\,l^{-1}$ buffered to neutral pH with sodium bicarbonate.

Molecular biology

All constructs were in the pTLN vector and were expressed by injecting 25–50 ng of cRNA transcribed from linearized cDNA using the CellScript AmpliCap^{TM} SP6 High Yield Message Maker Kit (CellScript Inc., Madison, WI, USA) or the mMessage mMachine kit (Ambion, Carlsbad, CA, USA). Mutations were introduced by recombinant PCR as described previously (Accardi & Pusch, 2003) and sequenced. Oocytes were kept in ND96 solution containing (in mM) 90 NaCl, 10 Hepes, 2 KCl, 1 $MgCl_2$, 1 $CaCl_2$, pH 7.5, for 3–6 days at 18°C.

Two-electrode voltage clamp

Two-electrode voltage clamp was performed with a Turbotec 03 amplifier (npi, Tamm, Germany) and the custom acquisition program GePulse (freely available at http://users.ge.ibf.cnr.it/pusch/programs-mik.htm). For measurements of stationary currents, the pulse protocol consisted of voltage steps of 50 ms from 120 to –80 mV in decrements of 20 mV. For measurements of tail currents, the pulse protocol consisted of a 30 ms pre-pulse to 100 mV, followed by a test pulse consisting of voltage steps of 30 ms from 120 mV to –100 mV in decrements of 10 mV, and a post-pulse of 30 ms to either 100 or –100 mV. Linear capacitive and leak currents were subtracted using the *P*/–*n* protocol. For measurements of the transient currents of E268A and D76H-E268A, the pulse protocol consisted of 10 ms voltage steps from 200 to –100 mV in 10 mV decrements. The holding potential was –30 mV. The standard extracellular solution contained 100 mM NaCl, 5 mM $MgSO_4$, 10 mM Hepes, pH 7.3. For experiments with anion substitution, NaCl was either entirely replaced by $NaNO_3$ or reduced by substitution of NaCl with Na-glutamate (with equimolar amounts). For solutions with different pH values, Hepes was replaced by Mes for pH < 7.3, glutamic acid for pH ≤ 4.8 and CAPS for pH > 8.3. Unless otherwise stated, measurements were performed at room temperature (20–25°C). For

measurements of the temperature dependence, the temperature of the bath solution was controlled by a custom-made temperature control system. Proton transport was qualitatively measured by monitoring the acidification of the extracellular solution close to the oocyte using a pH-sensitive microelectrode as described previously (Picollo & Pusch, 2005).

Patch clamp

Patch clamp measurements were performed on oocytes in the inside–out configuration. Pipettes were pulled from aluminosilicate capillaries (Hilgenberg, Malsfeld, Germany), coated with Sylgard (Dow Corning Corporation, Midland, MI, USA) and fire polished to a resistance of 0.5–1.5 MΩ. The extracellular (pipette) solution contained 100 mM *N*-methyl-D-glucamine (NMDG)-Cl, 10 mM Mes and 5 mM $MgCl_2$ (pH 5.8). The intracellular solution contained 100 mM NMDG-Cl, 10 mM Hepes, 2 mM $MgCl_2$ and 1 mM EGTA (pH 7.3). Hepes was replaced by Mes for the measurements performed at pH 5.3 and by CAPS for those performed at pH 9.3. Cl^- was reduced by substitution of NMDG-Cl with NMDG-Glu. The voltage protocol consisted of a 15 ms pre-pulse to 140 mV, followed by 15 ms steps from –120 mV to +140 mV in increments of 20 mV. The holding potential was 0 mV. Linear capacitive and leak currents were subtracted using the *P*/–*n* protocol with a holding potential at –30 mV. Currents were sampled at 50 kHz and the filter frequency was 10 kHz.

Analysis

Raw data were analysed using a custom analysis program (Ana; freely available at http://users.ge.ibf.cnr.it/pusch/programs-mik.htm) and the Origin program (OriginLab Corporation, Northampton, MA, USA). Two types of analysis of the inward currents were performed: on the tail currents generated by the test pulses to different voltages to analyse the dependence of the reversal potential of the currents on pH and $[Cl^-]$, and on the tail currents generated by the post-pulse to a constant voltage to analyse the voltage dependence of the gating process (as is typically performed on ion channels) as a function of pH. The analysis was performed by fitting the tail currents with a mono-exponential function and extrapolating the current magnitude at the onset of either the test pulse (to estimate the reversal potential) or the post-pulse (to estimate the voltage dependence of the gating process). Reversal potentials were calculated by interpolation of the three to four *I*–*V* data points closest to the zero current level with a second-degree polynomial function.

For the analysis of the voltage dependence of the inward tail currents, the *I*–*V* points obtained were fitted with a Boltzmann function of the form:

$$I(V) = I_{\min} + \frac{I_{\max} - I_{\min}}{1 + e^{z(V_{1/2}-V)F/(RT)}} \quad (1)$$

where $I_{\max}$ is the maximal current obtained at saturating voltages which was used to normalize the currents, $I_{\min}$ is the minimal current taking account of residual uncompensated leak, V is the voltage, $V_{1/2}$ is the voltage of half-maximal activation, z is the apparent gating valence and F, R and T are the Faraday constant, gas constant and absolute temperature, respectively. The normalization was performed at each pH with the maximal current at that specific pH obtained from the fit. This analysis allows direct information to be obtained about gating transitions in terms of the dependence of the probability of transport (analogous to the open probability of ion channels) as a function of the voltage of the test pulse.

The analysis of the temperature dependence of the inward tail currents was performed as indicated in SI Materials and Methods.

For the mutants E268A and D76H-E268A, charge–voltage (*Q*–*V*) relationships were derived as described previously (Zifarelli *et al.* 2012) (and Supplemental material) and fitted with a Boltzmann function of the form:

$$Q(V) = \frac{Q_{\max}}{1 + e^{z(V_{1/2}-V)F/(RT)}} \quad (2)$$

where V is the voltage, $V_{1/2}$ is the voltage of half-maximal activation, z is the apparent gating valence of the process, and F, R and T are the Faraday constant, gas constant and absolute temperature, respectively.

The theoretical dependence of the reversal potential on intracellular and extracellular $[Cl^-]$ and $[H^+]$, for transport mechanisms with different stoichiometry, was based on the general exchange reaction:

$$n\mathrm{Cl}^-_{\mathrm{ext}} + m\mathrm{H}^+_{\mathrm{in}} \rightleftharpoons n\mathrm{Cl}^-_{\mathrm{in}} + m\mathrm{H}^+_{\mathrm{ext}}$$

where n and m are the number of Cl^- and H^+ ions, respectively, transported in each cycle. The predicted reversal potential for this transport mechanism is given by V_{rev}:

$$\mathrm{V}_{\mathrm{rev}} = \frac{nE_{\mathrm{Cl}} + mE_{\mathrm{H}}}{n + m} \quad (3)$$

where E_{Cl} and E_{H} are the Nernst potentials for Cl^- and H^+, respectively (Accardi & Miller, 2004). Unless otherwise stated, error bars indicate SEM. Statistical differences were assessed using unpaired Student's t test.

Results

D76H shows inward tail currents at negative voltages

The aspartate residue at position 76 in ClC-5 is conserved in most CLC proteins (Fig. S1) and is spatially close to the conserved gating glutamate E211, probably accessible from the extracellular space (Fig. 1). We decided to investigate this residue because mutations of the corresponding aspartate in the CLC channels ClC-0 (D70G and D76E), ClC-1 (D136G) and ClC-Kb (D68N) drastically modified channel gating (Fahlke *et al.* 1995; Ludewig *et al.* 1997; Picollo *et al.* 2004). To explore the relevance of D76 for ClC-5 function, we investigated the effect of several amino acid substitutions (with C, E, G, H, K, N, Q, R and Y residues). With the exception of D76H, all the mutants gave currents very similar to WT, including the D76G mutation (Fig. S2), which has a strong effect when inserted in ClC-0 and ClC-1 (Fahlke *et al.* 1995; Ludewig *et al.* 1997). In contrast, the D76H mutant at neutral pH significantly slowed down the activation time course of the currents at positive voltages (Fig. 2). Even more interestingly, clear inward tail currents upon pulses to negative voltages could be observed at acidic pH after activation of the transporter (Fig. 2). For a detailed characterization of these inward tail currents of D76H, we applied a voltage protocol comprising a pre-pulse to 100 mV for maximal activation of the transporter prior to the test pulse, and analysed the pH and $[Cl^-]_{ext}$ of the tail currents (Figs 3 and 4). Importantly, no inward tail currents could be resolved for WT ClC-5 under any of the conditions tested (Figs 3 and 4).

The inward tail currents observed might reflect transmembrane ionic movements or could be transient capacitive currents originating from partial reactions in the transport cycle, similar to those seen for the proton glutamate mutant E268A (Smith & Lippiat, 2010; Zifarelli *et al.* 2012). In order to distinguish between these possibilities, we first compared the behaviour of WT ClC-5 with the D76H mutant for pH_{ext} ranging from 4.3 to 8. Figure 3 shows representative traces of both the D76H mutant and WT ClC-5 at some of the pH values tested. Interestingly, inward tail currents became progressively more pronounced on lowering the pH values to 5.3, whereas more acidic pH decreased the magnitude of both positive steady-state currents and inward tail currents, an effect that could be a result of the known pH-dependent inhibition of transport activity of ClC-5 at acidic pH (Friedrich *et al.* 1999). The reversal potential (V_{rev}) calculated at pH 5.3 is 20 ± 2 mV and is in good agreement with the value of around 18 mV expected for a Cl^-/H^+ antiporter with a 2 : 1 stoichiometry assuming a $[Cl^-]_{int}$

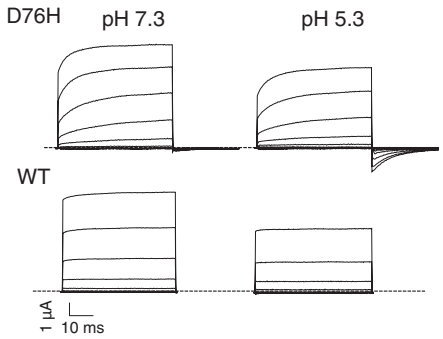

Figure 2. pH dependence of D76H and WT
Representative current recordings for D76H (upper traces) and WT ClC-5 (lower traces) at pH 7.3 and 5.3. Voltages of the test pulse ranged from 120 to –80 mV. Here and in all figures with current traces, the dashed line represents the zero current level.

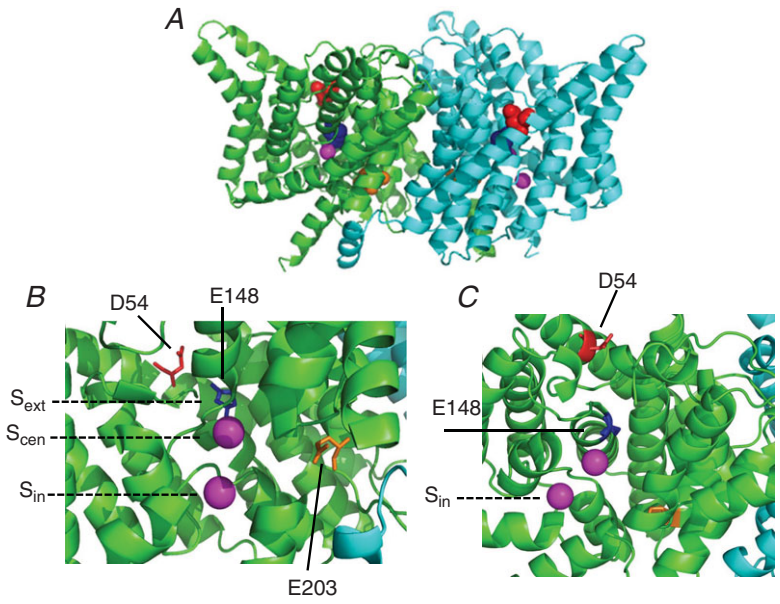

Figure 1. Location of the residue D76 mapped on the structure of ClC-ec1 (PDB entry: 1OTS)
A, dimeric structure of ClC-ec1 viewed from the membrane plane (extracellular side above and cytoplasmic side below). The two subunits are shown in green and cyan. Residue E148 (corresponding to E211 in ClC-5) is coloured in blue, D54 (corresponding to D76 of ClC-5) is shown in red and E203 (corresponding to E268 of ClC-5) in orange. Cl^- anions bound to S_{cen} and S_{int} are shown in magenta. *B*, expanded representation of the anion permeation pathway for one of the subunits. The position of the three binding sites, S_{ext}, S_{cen} and S_{int}, is also indicated by horizontal dashed lines. *C*, same representation as in *B* with a top view perpendicular to the membrane. In *B* and *C*, some transmembrane helices were removed for clarity.

value of 30 mM and pH_{int} of 7.3. For the quantitative analysis of the shift of the reversal potential at the different pH values, we subtracted from the reversal potential value measured for each pH the one measured at pH 5.3, obtaining ΔV_{rev} (Fig. 5*A*). The mean values of ΔV_{rev} depend linearly on pH_{ext} with a slope of around 20 mV per pH unit. The lines in Fig. 5*A* represent the theoretical values predicted for the shift of ΔV_{rev} in the case of a transporter with a 3 : 1 (dashed–dotted line), 2 : 1 (full line) and 1 : 1 (dashed line) Cl^-/H^+ stoichiometry and for a pure H^+ conductance (dotted line) (eqn (3)). We next investigated the dependence of the reversal potential on $[Cl^-]_{ext}$ (Fig. 4), keeping the pH_{ext} value at 5.3 to maximize the inward tail current magnitude. The shift of the reversal potential is shown in this case as the difference between the value of the reversal potential at each $[Cl^-]_{ext}$ and the value measured at 100 mM Cl^-. Taken together, these experiments clearly rule out the possibility that the mutant D76H behaves as a purely diffusive Cl^- conductance (dotted lines in Fig. 5*A* and *B*), but they do not allow a modified transport stoichiometry compared with WT to be unambiguously ruled out. To further clarify this point and also to investigate whether the tail currents depend specifically on the extracellular pH and Cl^- concentrations, or whether they depend in general on the transmembrane H^+ and Cl^- concentration gradients, we performed patch clamp experiments to vary also the composition of the intracellular solutions. For these measurements $[Cl^-]_{ext}$ was 110 mM and the external pH_{ext} was fixed at 5.8, because patch stability was problematic at pH 5.3. Sample traces from three different representative patches obtained at the three internal pH values tested (5.3, 7.3 and 9.3) are shown in Fig. 6*A*. At pH_{int} 7.3 (Fig. 6*A*), but also at $[Cl^-]_{int}$ = 104 mM (Fig. 7*A*), currents activated by the pre-pulse to 100 mV did not reach saturation. However, we found it problematic to prolong the pre-pulse length without compromising patch stability. Indeed, the voltage protocol was already quite long as a result of the application of a *P*/–*n* protocol and the need to average traces to reduce noise. The small inward tail currents at pH_{int} 5.3 preclude the measurement of the reversal potential, but their magnitude increases at pH 7.3 and 9.3 (Fig. 6*A*). In this case the shift of the reversal potential measured at pH 7.3 and 9.3 is in very good agreement with the values expected for a $2Cl^- : 1H^+$ exchanger (Fig. 6*B*, full line) and not with the values expected for different stoichiometries (3 : 1 or 1 : 1, dashed–dotted and dashed lines, respectively). Inward tail currents also depend on $[Cl^-]_{int}$. They were larger at 104 mM $[Cl^-]_{int}$ than at 21 mM $[Cl^-]_{int}$ (Fig. 7*A*), and the measured reversal potentials match only with the theoretical values expected for a $2Cl^- : 1H^+$ exchanger (Fig. 7*B*, full line). Thus, the dependence of the reversal potential of D76H tail currents on external and internal $[Cl^-]$ and pH collectively demonstrates that the tail currents reflect ionic transmembrane transport of Cl^- towards the extracellular space and of H^+ in the opposite direction with a $2Cl^- : 1H^+$ stoichiometry. To directly assess whether the D76H mutation alters the proton transport activity associated with outward currents, we also compared the degree of extracellular acidification produced by the activation of stationary currents at 80 mV of WT and mutant ClC-5 using a pH-sensitive microelectrode (Picollo & Pusch, 2005). Like WT, activation

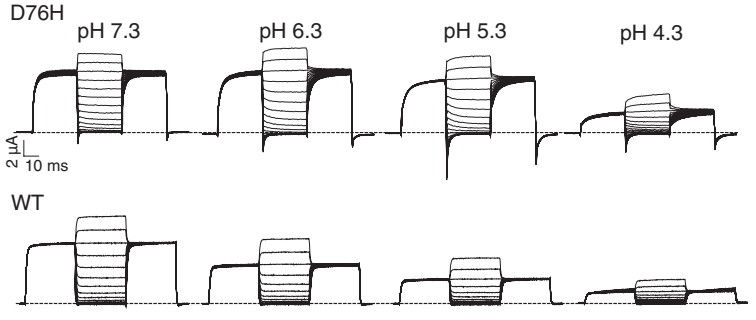

Figure 3. pH dependence of inward tail currents
Representative current recordings for D76H (upper traces) and WT ClC-5 (lower traces) at some of the pH_{ext} values tested (7.3, 6.3, 5.3, 4.3), obtained with a voltage protocol comprising a pre-pulse and a post-pulse to 100 mV.

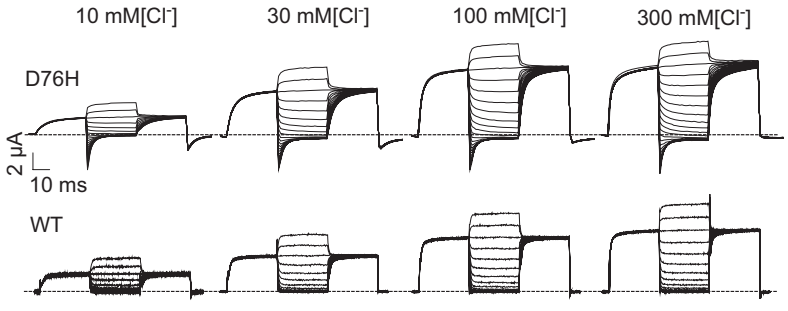

Figure 4. Chloride dependence of inward tail currents
Representative current recordings for D76H (upper traces) and WT ClC-5 (lower traces) at different $[Cl^-]_{ext}$ (10, 30, 100 and 300 mM). pH_{ext} is 5.3.

of D76H leads to a robust extracellular acidification that is fully reversible (Fig. S3*A*), and the ratio of outward currents to the degree of acidification, e_{rel} (Supplemental material eqn (1)), is quantitatively very similar to that measured for WT (Fig. S3*B*).

The inward tail currents are compatible with a conformational change

To test whether the inward tail currents are compatible with a conformational change of the transporter, we assessed the dependence of the tail current's kinetics on temperature. Experiments were performed with the voltage clamp technique at pH_{ext} 5.3 at temperatures of 10, 15 and 22°C (Fig. S4*A*). Tail currents at –120 mV could be fitted by a double-exponential function (Fig. S4*A*). The fast time constant (on the order of 0.5 ms) probably reflects residual uncompensated oocyte capacitance and is basically independent of temperature. The slower time constant, τ_{slow}, shows exponential temperature dependence (Fig. S4*B*, full line) and provides an estimate of the temperature coefficient (Q_{10}) of 2.88 ± 0.03 (Supplemental material eqn (3)).

Tail currents mirror voltage- and pH-dependent gating

The tail currents mediated by D76H demonstrate that the transporter undergoes a gating process and allow, for the first time, reliable quantification of its voltage dependence. To this aim we applied two different pulse protocols, with a post-pulse to 100 and –100 mV, respectively. The tail currents at these potentials were fitted with a mono-exponential function to extrapolate the amplitude of the currents to the onset of the post-pulse. Figure S5 shows that the two protocols provide very similar results at pH 5.3. However, because currents at the post-pulse to –100 mV became too small at basic pH values, we employed the protocol with the post-pulse to 100 mV to extract quantitative gating parameters. Figure 8 shows the dependence of the normalized inward tail currents on pH_{ext} which basically represents the probability that ClC-5 is in a transport-competent state. The values obtained were used to construct the voltage dependence of the gating process as a function of pH as shown for a representative oocyte in Fig. 8*B*. Data points were fitted with a Boltzmann function (eqn (1)) to derive $V_{1/2}$ and z of the gating process. Mean values of $V_{1/2}$ were 27.7 ± 3.9 (pH 7.3), 53.9 ± 4.6 (pH 6.8), 60.4 ± 6.9 (pH 6.3), 88.9 ± 12.6 (pH 5.8), 86.4 ± 5.6 (pH 5.3), 108.9 ± 2.9 (pH 4.8) and 134 ± 9.2 (pH 4.3), with a progressive right shift of $V_{1/2}$ at more acidic pH values (Fig. 8*C*), and a linear pH dependence with a slope of 30.7 ± 6.4 mV per pH unit. An element that further supports the validity of our conclusion about the presence of a gating process is the analysis shown in Fig. S8. The I–V relation measured for the stationary currents is in excellent agreement with the theoretical relationship obtained by multiplying the values of the instantaneous currents by the probability that ClC-5 is in a transport-competent state derived from the tail current analysis (see also legend of Fig. S8). Interestingly,

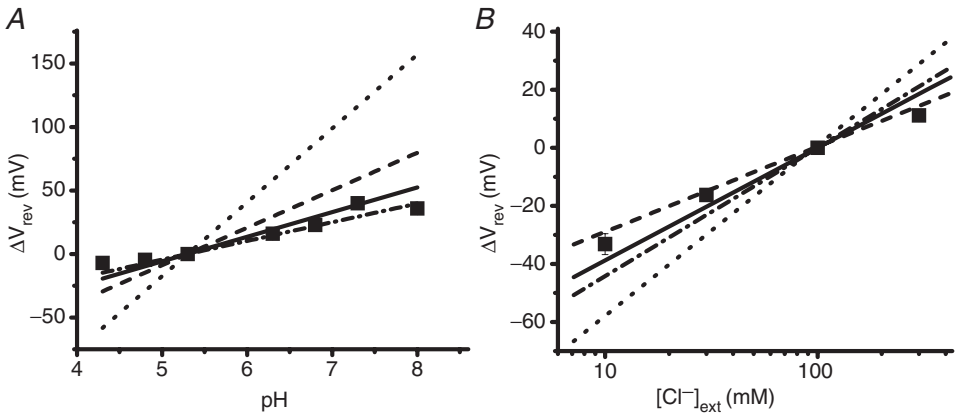

Figure 5. Dependence of the inward tail currents of D76H on pH_{ext} and $[Cl^-]_{ext}$
A, changes in the reversal potential as a function of pH_{ext} are presented as ΔV_{rev}, obtained as the difference between the reversal potential value at each pH and the value obtained at pH 5.3. Data are presented for pH 4.3 ($n = 7$), 4.8 ($n = 7$), 5.3 ($n = 12$), 6.3 ($n = 5$), 6.8 ($n = 5$), 7.3 ($n = 5$) and 8 ($n = 6$). Measurements were performed at 100 mM $[Cl^-]_{ext}$. The full, dashed-dotted, dashed and dotted lines represent the theoretical expectation for the changes in the reversal potential for transporters with 2 : 1, 3 : 1 or 1 : 1 Cl^-/H^+ stoichiometry or a pure proton conductance, respectively, under the same pH conditions. ΔV_{rev} values calculated do not depend on assumptions on $[Cl^-]_{int}$ (eqn (3)). *B*, the reversal potential as a function of $[Cl^-]_{ext}$ is presented as the difference between the reversal potential value at each Cl^- concentration and the value obtained at 100 mM $[Cl^-]$. Data are presented for $[Cl^-]$ of 10 mM ($n = 8$), 30 mM ($n = 7$), 100 mM ($n = 7$) and 300 mM ($n = 6$). Full, dashed-dotted, dashed and dotted lines have the same meaning as in *A*. ΔV_{rev} values calculated do not depend on assumptions on pH_{int} (eqn (3)). Error bars are mostly smaller than symbols.

the instantaneous currents show pronounced rectification at neutral pH, whereas they are much less rectifying at acidic pH (see also Discussion).

Transient currents of D76H–E268A and E268A

The results described above indicate that the inward tail currents of D76H originate from a gating mechanism that regulates the transport currents. However, we sought an independent approach to confirm this conclusion. To this aim we took advantage of another ClC-5 mutant, E268A, which elicits transient currents, but with very different functional properties compared with D76H (Smith & Lippiat, 2010; Zifarelli *et al.* 2012). In contrast with D76H, E268A abrogates stationary currents, and it has been suggested that, for E268A, transient currents originate from charge movement associated with partial reactions in the transport cycle rather than from the presence of a gating mechanism (Zifarelli *et al.* 2012). Therefore, we reasoned that, if the double mutant D76H–E268A shows transient currents that are similar to the single E268A mutant, this would provide additional evidence for the idea that the transient inward currents observed for D76H originate from gating of the transport current. Figure 9*A* shows recordings from one oocyte at various $[Cl^-]_{ext}$ for E268A and D76H–E268A, and suggests that transient currents are very similar for the two constructs. In order to perform a more quantitative analysis, we integrated the charge moved during the transients according to the procedure already performed by Zifarelli *et al.* (2012), obtaining *Q*–*V* relationships that were fitted by a Boltzmann function (eqn (2)). Reducing $[Cl^-]_{ext}$ progressively shifts $V_{1/2}$ to more positive values and reduces the maximal gating charge obtained at 200 mV in an almost identical manner for E268A and D76H–E268A (Fig. 9*B* and *C*). We also compared the pH dependence of transient currents of E268A and D76H–E268A. Figure S6*A* shows recordings from one oocyte at various external pH values for E268A and D76H–E268A. As reported previously for E268A (Zifarelli *et al.* 2012), varying pH_{ext} from 5.3 to 9 has only relatively small effects on the transient currents and on the resulting values of $V_{1/2}$ and z of the *Q*–*V* relationship for E268A (Fig. S6*B* and *C*). The double mutant D76H–E268A is very similar to E268A (Fig. S6). Thus the presence of the D76H mutation in the background of E268A does not influence the transient currents elicited by E268A alone. From this it can safely be concluded that, when normal transport activity is abrogated as in the E268A background, D76H is unable to generate inward tail currents, and this is consistent with the idea that the inward tail currents observed for D76H are caused by a gating mechanism.

We also investigated whether NO_3^-, which produces a partial uncoupling of the transport mechanism of ClC-5 (Nguitragool & Miller, 2006; Zdebik *et al.* 2008; Zifarelli & Pusch, 2009), would also affect gating of D76H. Upon substitution of Cl^-_{ext} with NO_3^-, the outward currents increased (Fig. S7*A* and *B*), an effect that has already been thoroughly investigated (De Stefano *et al.* 2011). However, the inward tail currents at voltages more negative than 0 mV remained very similar in magnitude

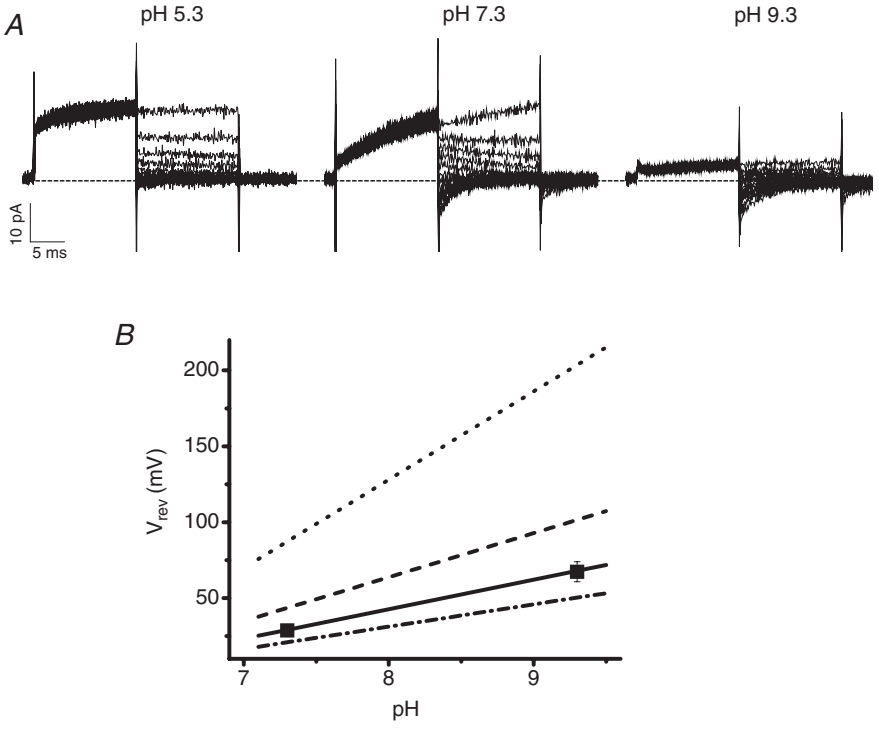

Figure 6. Dependence of the inward tail currents on pH_{int}
A, representative inward tail currents at the indicated pH_{int} values (5.3, 7.3, 9.3) from three different oocytes. $[Cl^-]_{ext}$ is 110 mM and pH_{ext} is 5.8. Currents shown are the average of five traces. *B*, mean values of the reversal potential at pH_{int} 7.3 ($n = 5$) and 9.3 ($n = 3$). The full, dashed-dotted, dashed and dotted lines represent the theoretical expectation for the changes in the reversal potential for transporters with a 2 : 1, 3 : 1 or 1 : 1 Cl^-/H^+ stoichiometry or a pure proton conductance, respectively, derived from eqn (3).

and kinetics (Fig. S7*C*). In principle this finding may not be surprising, because the inward tail currents reflect an outward movement of anions, whose concentrations are unaltered by the exchange of extracellular Cl^- with NO_3^-. However, keeping in mind the relatively slow time resolution of voltage clamp measurements, this finding suggests that ClC-5 switches 'instantaneously' between uncoupled transport in the presence of NO_3^- and coupled transport in the presence of Cl^-.

Discussion

ClC-5 is a $2Cl^-/1H^+$ antiporter highly expressed in endosomes of proximal tubule cells of the kidney, where it is critical for proper endocytosis (Stauber *et al.* 2012). However, the properties of ClC-5 in its physiological localization, the endosomal membrane, have never been directly assessed and, in general, the mechanisms underlying vesicular ion homeostasis are far from clear. In this scenario, the physiological role of ClC-5 is still controversial and one of the most prominent problems is whether the strong rectification of ClC-5 currents observed on expression in heterologous systems is preserved when ClC-5 is expressed in endosomes, and what is the mechanism generating this behaviour, a question that so far has remained unanswered.

In this work we identified a ClC-5 mutant, D76H, which, besides currents in the positive voltage range, also mediates inward tail currents at negative potentials after an activating positive voltage step. The rationale behind the choice to mutate this residue was based on previous studies investigating mutations of the corresponding aspartate residue in ClC-0 (D70G and D76E), ClC-1 (D136G) and ClC-Kb (D68N) (Fahlke *et al.* 1995; Ludewig *et al.* 1997; Picollo *et al.* 2004). For these CLC channels, mutations of this conserved residue drastically modified channel gating, affecting mostly the currents elicited by negative potentials which, in contrast with WT, became slowly activating producing, in ClC-0 and ClC-1, a strong inward rectification (Fahlke *et al.* 1995; Ludewig *et al.* 1997). However, in ClC-5, the mutation D76G did not have an effect as observed with the substitutions with C, E, K, N, Q, R and Y. Importantly, in comparison with WT ClC-5, the D76H mutant is characterized by much slower activation and deactivation of the currents, giving rise to inward tail currents at negative potentials. Thus, D76H is the first mutation that confers upon ClC-5 the ability to transport Cl^- out of and H^+ into the cell, albeit only transiently, and therefore to measure the reversal potential of ClC-5-mediated transport under a variety of conditions, confirming our earlier finding of a $2Cl^- : 1H^+$ stoichiometry (Zifarelli & Pusch, 2009). More importantly, the properties of the mutant demonstrate unambiguously the presence of a gating process that underlies, at least in part, the strong outward rectification of ClC-5. In fact, we could definitely exclude that the inward tail currents of D76H represent capacitive transient currents generated by partial reactions of the transport cycle. This conclusion is based on several lines of evidence. In particular, the dependence on intracellular and extracellular pH and $[Cl^-]$ of the inward tail currents demonstrates that they reflect ionic transmembrane transport with a $2Cl^- : 1H^+$ stoichiometry, just like the steady-state transport stoichiometry observed for WT ClC-5 at positive potentials (Zifarelli & Pusch, 2009). Moreover, outward stationary currents mediated by D76H have a similar voltage dependence, show a qualitatively similar inhibition at acidic pH and are associated with a qualitatively similar proton transport activity to WT. This indicates that general transport properties are not altered in D76H, supporting the notion that the mutant specifically alters gating kinetics and does not introduce major additional pH-dependent processes. Based on these considerations, it is reasonable to assume that the basic features of the gating mechanism investigated in this work on the mutant D76H are conserved in WT ClC-5.

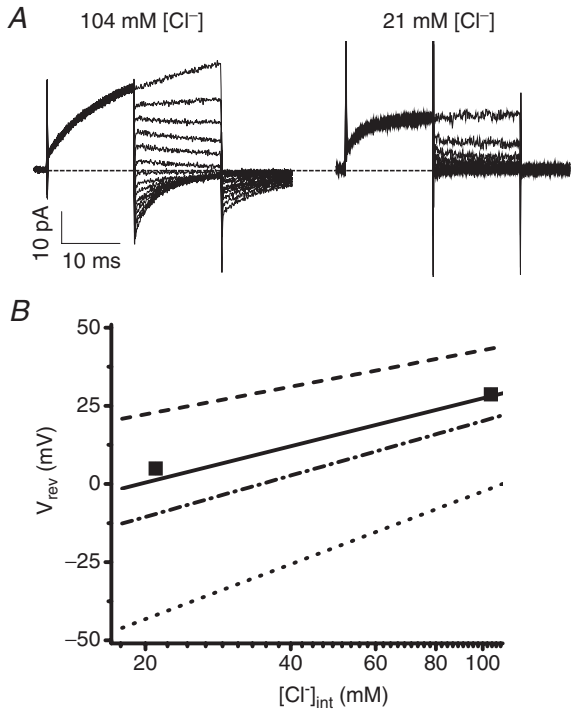

Figure 7. Dependence of the inward tail currents on $[Cl^-]_{int}$
A, representative inward tail currents at the indicated $[Cl^-]_{int}$ (104 and 21 mM). $[Cl^-]_{ext}$ is 110 mM and pH_{ext} is 5.8. Currents shown are the average of five traces. *B*, mean values of the reversal potential at $[Cl^-]_{int}$ = 104 ($n = 5$) and 21 mM ($n = 4$). The full, dashed-dotted, dashed and dotted lines represent the theoretical expectation for the changes in the reversal potential for transporters with a 2 : 1, 3 : 1 or 1 : 1 Cl^-/H^+ stoichiometry or a pure proton conductance, respectively, derived from eqn (3). Error bars are smaller than symbols.

We obtained further support for the conclusion that inward tail currents of D76H are caused by a gating mechanism by comparing transient currents observed for the 'proton glutamate' mutation E268A with those of the double mutant D76H–E268A. Mutant E268A abrogates stationary transport and presents transient currents that most probably originate from partial reaction in the transport cycle (as this mutant is unable to complete a full transport cycle). Thus, we reasoned that, if D76H tail currents are a result of transporter gating, they should not appear if D76H is inserted in the background of E268A. The almost identical behaviour of E268A and D76H–E268A indicates that D76H selectively alters the gating mechanism of the transporter, but not the intrinsic transport mechanism. Vice versa, this result reinforces our earlier conclusion that the transient currents of E268A reflect a partial reaction cycle (Zifarelli *et al.* 2012). This conclusion and, in general, the findings of this work can be illustrated by considering a hypothetical schematic model (Fig. 10) showing how a gating mechanism might potentially regulate the transport activity of ClC-5. The gating mechanism might control the transition of ClC-5 from the inactive state I, where it is unable to transport, to one of the states of the transport cycle, allowing transport activity. Our results indicate that the gating transitions are voltage and pH dependent. Importantly, the model predicts that the overall voltage dependence of ClC-5 macroscopic currents depends on both the voltage dependence of this gating process and that associated with partial reactions of the transport cycle. This is relevant considering that we found the probability of being in a transport-competent state to be surprisingly left-shifted ($V_{1/2}$ around 20 mV) compared with the voltage dependence of the stationary currents of ClC-5. This could be a result of the fact that very fast gating components cannot be resolved in our measurements and lead to an overestimate of this probability. This would be consistent with the analysis shown in Fig. S8, where we compare the voltage dependence of the stationary currents and of the instantaneous currents (obtained after an activating pre-pulse), and also derive the theoretical values of the stationary currents expected from the instantaneous currents and the gating parameters. The figure shows that we could faithfully reproduce the values of the stationary currents, supporting our conclusion about the presence of

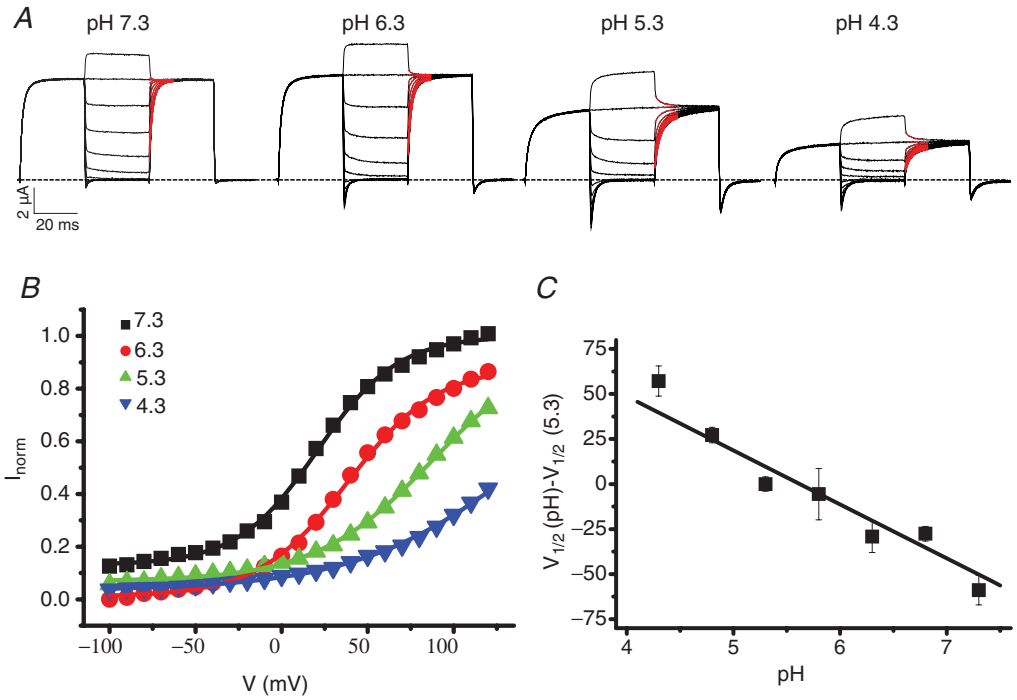

Figure 8. Voltage dependence of gating of D76H as a function of pH_{ext}
A, representative current traces at the indicated pH_{ext} from one oocyte. Red lines represent the mono-exponential fit of the tail currents elicited by a post-pulse to 100 mV. The amplitude of the tail currents at the onset of the post-pulse was extrapolated from the fit. These values were normalized with the parameter I_{max} derived from the fit with eqn (1) to obtain the current–voltage (*I–V*) relationships. *B*, *I–V* relationships for the oocyte shown in *A*. Full lines are the fit of the data with a Boltzmann function (eqn (1)) providing estimates for $V_{1/2}$ and *z* of 21, 39, 89, 141 mV and 1.1, 1.0, 0.8 and 0.5, respectively, for pH 7.3, 6.3, 5.3 and 4.3. *C*. mean values of the difference between $V_{1/2}$ calculated at pH 4.3 ($n = 6$), 6.3 ($n = 5$), 7.3 ($n = 7$) and that calculated at pH 5.3 ($n = 10$) as a function of pH_{ext}. The full line represents the fit of the data with a linear function with a slope of 30.7 ± 6.4 per pH unit.

a gating mechanism in ClC-5 and the internal consistency of our measurements. Importantly, the instantaneous inward currents at neutral pH are very small, i.e. they are almost as rectifying as the stationary currents, compatible with gating kinetics that are fast enough to re-equilibrate in a few microseconds and too fast to be resolved. However, at more acidic pH values, the instantaneous currents are much less rectifying, which is compatible with slower gating kinetics that allow their temporal resolution after the pre-pulse; in this case the transport activity (of the fully activated ClC-5) depends more linearly on voltage. This implies that ClC-5 rectification would be conferred exclusively by the voltage dependence of the gating mechanism, similar to the conclusion drawn for ClC-7 (Leisle *et al.* 2011). This interpretation is also consistent with the idea that this gating process becomes apparent in the D76H mutant because of slower kinetics compared with WT, not only at negative but also at positive voltages. However, our data are equally consistent with the interpretation that the strong rectification of ClC-5 currents is not only caused by the gating mechanism, but also by a contribution of the transport cycle itself if the turnover rate is non-linearly dependent on voltage. Distinction between these possibilities requires a direct investigation of the voltage dependence of the turnover rate, which implies strict control of the gating mechanism (in order to exclude effects of its voltage dependence), thus posing the same problem as for the alternative interpretation.

The model also illustrates that the mutant E268A is confined to a limited branch of the transport cycle indicated by the shaded box. Therefore, the properties of the transient currents of E268A reflect those confined reactions in the transport cycle and do not recapitulate the voltage and pH dependence of the entire transport cycle or of the gating transition to the inactive state I. In particular, from the almost identical behaviour of E268A and D76H–E268A, it can be concluded that the mutation D76H does not have a significant influence on the partial reactions 'explored' by E268A. Thus, given that the transient currents of E268A and the tail currents of D76H reflect different processes (partial reactions of the transport cycle *versus* gating of the transport activity), it is not surprising that they show different pH-dependent properties and voltage dependence. It is important to note that this model anticipates a certain degree of coupling between transport activity and gating because the transition to state I probably depends on the occupation of

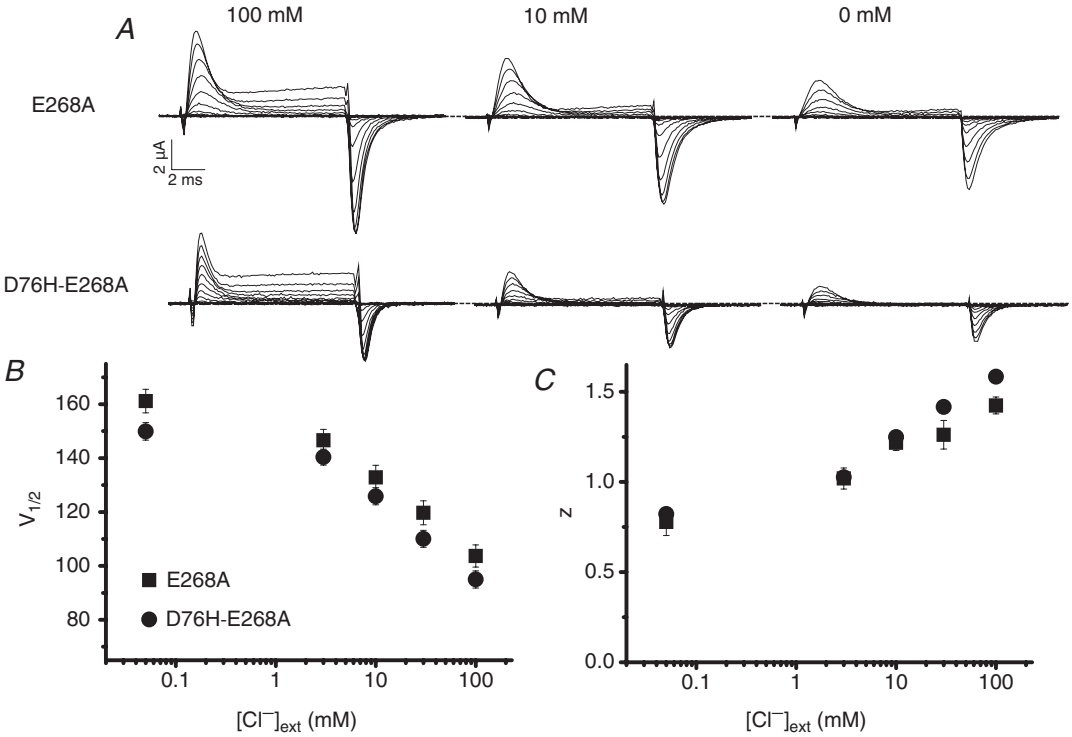

Figure 9. Comparison of the transient currents of E268A and D76H–E268A at different $[Cl^-]_{ext}$
A, representative current recordings from two oocytes, one expressing E268A (upper panel) and one expressing D76H–E268A (lower panel) at the indicated $[Cl^-]_{ext}$. *B* and *C*, average values for $V_{1/2}$ and z, respectively, obtained from the Boltzmann fit of the Q–V relationship for $[Cl^-]_{ext}$ of 0 mM (a contaminating concentration of 80 μM was assumed, see Zifarelli *et al.* 2012) ($n = 6$), 3 mM ($n = 7$), 10 mM ($n = 6$), 30 mM ($n = 7$) and 100 mM ($n = 6$) (eqn (3) and Supplemental material).

the various states of the transport cycle. The presence of a gating mechanism for CLC antiporters has been convincingly demonstrated so far only for ClC-7 (Leisle *et al.* 2011), whereas for ClC-4 and ClC-5 the evidence was less conclusive (Zdebik *et al.* 2008; Alekov & Fahlke, 2009; Orhan *et al.* 2011). Zdebik *et al.* (2008) suggested that ClC-5 is a gated transporter on the basis of spectral analysis of the noise that had the typical features of the Lorentzian spectrum observed for ion channel noise. Studies on the gating mechanism of ClC-4 could not resolve inward tail currents and, were mostly performed in the presence of uncoupling anions that drastically modify the canonical transport mechanism (Alekov & Fahlke, 2009; Orhan *et al.* 2011). In addition, Orhan *et al.* performed also measurements with Cl^- as the only anion present and interpreted outward current relaxation (Fig. 5 in Orhan *et al.*) as reflecting a gating mechanism regulating ClC-4 transport (Orhan *et al.* 2011). However, the resulting high transport probability (0.6–0.7) at negative potentials appears difficult to reconcile with the transport properties of ClC-4. With regard to the effect of uncoupling anions, it is interesting to note that the similar amplitude and kinetics of the inward tail currents in the presence of extracellular Cl^- and NO_3^- observed in this work allow us to conclude that ClC-5 can instantaneously (with the time resolution provided by the voltage clamp measurements) switch between uncoupled transport in the presence of NO_3^- and coupled transport in the presence of Cl^-. This supports the notion that the transition between uncoupled and coupled transport apparently requires only the displacement of bound NO_3^- by the intracellular Cl^- transported. The fast transition between uncoupled and coupled transport is consistent with previous observations on ClC-4 (Alekov & Fahlke, 2009), and indicates that it is not necessary to postulate that the uncoupling observed in the presence of NO_3^- is associated with a major (and possibly slow) conformational change of the protein. In this respect, it could also be interesting to study the effect on ClC-5 of anionic buffers, such as bicarbonate and phosphate, that could be more directly related to its physiological role in the kidney.

For ClC-7 the presence of a gating mechanism was indicated by the presence of slowly deactivating inward currents (Leisle *et al.* 2011), and it has been found recently that this gating involves the interaction of the two subunits similar to the common gating of ClC-0 (Ludwig *et al.* 2013). Patch clamp experiments performed in HeLa cells expressing the R762Q mutant of ClC-7 at neutral pH indicated a gating mechanism characterized by values of $V_{1/2}$ and z of 81 mV and 1.32, respectively (Leisle *et al.* 2011), whereas, for ClC-5, we found values of 21 mV and 1.1. Thus, the gating mechanisms of ClC-5 and ClC-7 appear to have a comparable apparent gating charge, but a different voltage dependence. This might be explained by the presence of fast gating components already discussed, but might also reflect specific properties of the two transporters. Indeed, although ClC-5 and ClC-7 share, in general, a similar transport mechanism (stoichiometry, inhibition by acidic pH, residues involved in transport coupling) (Jentsch, 2008; Leisle *et al.* 2011), they also differ in a number of properties, such as kinetics of transport currents, cellular localization and need for ClC-7 to mutate lysosomal sorting motifs and associate with Ostm1 for functional plasma membrane expression, which might underlie the different voltage dependence of gating. Considering also

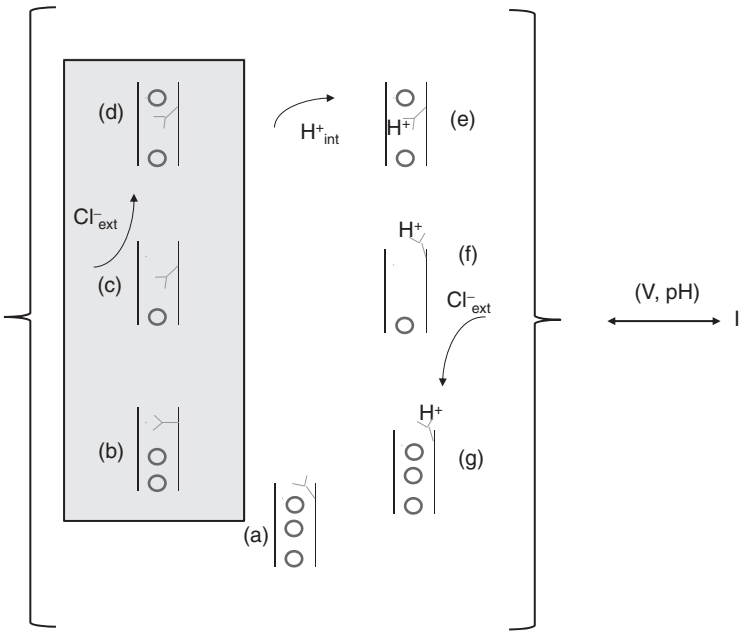

Figure 10. Schematic model of the transport cycle of ClC-5 including a gating mechanism
The hypothetical model is based on the transport cycle suggested for ClC-Cm by Feng *et al.* (2010) with the addition of state (c). The model is not intended to provide a realistic description of the ClC-5 transport cycle, but rather to guide a mechanistic interpretation of the results. Circles represent Cl^- ions; the shaded box represents the branch of the transport cycle that is accessible to the E268A mutant. From any of the states composing the transport cycle, indicated collectively by a brace, ClC-5 can transition to the inactive state I in which it is not able to transport. Forward and backward transitions to state I are voltage and pH dependent. In state (a), the side chain of E211 is unprotonated and the transporter has all the binding sites occupied by Cl^- ions. In state (b), the side chain of E211 moves to occupy S_{ext} and one Cl^- ion moves intracellularly. In state (c), the side chain of E211 moves to occupy S_{cen} and this is associated with the transport of another Cl^- ion, whereas S_{ext} is transiently empty but binds an extracellular Cl^- ion in state (d). From this conformation E211 can be protonated by an intracellular proton (state e) and can move outwardly (state f), giving way to Cl^- binding from the extracellular space (state g).

that, for ClC-7, the dependence of gating on pH was not directly investigated (Leisle *et al.* 2011), the relationship between the gating of ClC-5 and ClC-7 requires further investigation.

ClC-5 currents are inhibited by acidic pH_{ext} (Friedrich *et al.* 1999). Picollo *et al.* (2010) proposed that this inhibition can be entirely explained by a voltage-dependent H^+ block of transport activity, i.e. turnover, but these authors did not consider possible effects of pH on ClC-5 gating. Here, we found that gating of ClC-5 appears to depend strongly on pH_{ext}, with acidic values that progressively shift the voltage dependence of gating towards positive potentials (Fig. 8). This indicates that the inhibition of ClC-5 currents at acidic pH is caused, at least in part, by the effect of pH on gating. However, unraveling the effect of H^+ on transport and gating would require a direct estimate of the turnover rate of the transporter, a result that requires significant technical progress. Intriguingly, the inhibitory effect of pH_{ext} on ClC-5 gating is qualitatively similar to that observed for ClC-4 in uncoupling conditions (Orhan *et al.* 2011), but opposite to the effect on the CLC channels ClC-0 and ClC-1, where acidic pH promotes channel opening (Rychkov *et al.* 1996; Chen & Chen, 2001).

To establish whether the gating observed for ClC-5 bears any relation with the gating of CLC channels, we assayed the dependence of the inward currents on temperature and found $Q_{10} \sim 3$, very similar to the value found by Leisle *et al.* (2011) for the antiporter ClC-7. CLC Cl^- channels have two kinds of gates, the 'protopore gate' and the 'common gate'. In ClC-0, the protopore gate is fast and has $Q_{10} \sim 2.2$, whereas the common gate is slow with $Q_{10} \sim 40$ (Pusch *et al.* 1997). However, protopore and common gates of the muscle Cl^- channel ClC-1 have Q_{10} values of ~3 and ~4, respectively (Bennetts *et al.* 2001). Thus, the Q_{10} value found here is compatible with a conformational change that appears qualitatively similar to that observed in other CLC channels and transporters, but much smaller than that which probably characterizes the slow gate in ClC-0.

We are unable to propose any kind of structural mechanism by which the D76H mutation could slow down ClC-5 gating kinetics generating inward tail currents, and why this effect is specific to the histidine substitution. In any case, it is interesting to note that this effect bears some similarity to that produced by mutations of the corresponding residue in ClC-0 and ClC-1 (Fahlke *et al.* 1995; Ludewig *et al.* 1997), suggesting an important and, to some extent, conserved role of this residue for the gating of CLC proteins.

With regard to the general relevance of our results for the family of CLC transporters, the presence of a gating mechanism, shown in this work for ClC-5 (closely related to ClC-3 and ClC-4) and ClC-7 (closely related to ClC-6) (Leisle *et al.* 2011), might suggest that this is a conserved feature for CLC transporters, although the specific gating properties might differ.

In conclusion, we identified a ClC-5 mutation that elicits inward tail currents in the negative voltage range, allowing the bidirectional coupled transport of Cl^- and H^+. Our results indicate that the inward currents are caused by the relaxation of a gating mechanism in ClC-5, directly demonstrated in this work for the first time, although it remains to be elucidated whether fast gating components not resolved in this study are also present. This gating mechanism is dependent on both voltage and pH_{ext}, and contributes to the extreme rectification of WT ClC-5.

These results provide an important step forward in our understanding of the biophysical basis of CLC transporter function with potentially relevant implications for the physiological role of ClC-5 *in vivo*.

References

Accardi A, Kolmakova-Partensky L, Williams C & Miller C (2004). Ionic currents mediated by a prokaryotic homologue of CLC Cl^- channels. *J Gen Physiol* **123**, 109–119.

Accardi A & Miller C (2004). Secondary active transport mediated by a prokaryotic homologue of ClC Cl^- channels. *Nature* **427**, 803–807.

Accardi A & Pusch M (2003). Conformational changes in the pore of CLC-0. *J Gen Physiol* **122**, 277–293.

Accardi A, Walden M, Nguitragool W, Jayaram H, Williams C & Miller C (2005). Separate ion pathways in a Cl^-/H^+ exchanger. *J Gen Physiol* **126**, 563–570.

Alekov AK & Fahlke C (2009). Channel-like slippage modes in the human anion/proton exchanger ClC-4. *J Gen Physiol* **133**, 485–496.

Bennetts B, Roberts ML, Bretag AH & Rychkov GY (2001). Temperature dependence of human muscle ClC-1 chloride channel. *J Physiol* **535**, 83–93.

Chen MF & Chen TY (2001). Different fast-gate regulation by external Cl^- and H^+ of the muscle-type ClC chloride channels. *J Gen Physiol* **118**, 23–32.

De Stefano S, Pusch M & Zifarelli G (2011). Extracellular determinants of anion discrimination of the Cl^-/H^+ antiporter protein CLC-5. *J Biol Chem* **286**, 44134–44144.

Drummond GB (2009). Reporting ethical matters in *The Journal of Physiology*: standards and advice. *J Physiol* **587**, 713–719.

Dutzler R, Campbell EB, Cadene M, Chait BT & MacKinnon R (2002). X-ray structure of a ClC chloride channel at 3.0 Å reveals the molecular basis of anion selectivity. *Nature* **415**, 287–294.

Dutzler R, Campbell EB & MacKinnon R (2003). Gating the selectivity filter in ClC chloride channels. *Science* **300**, 108–112.

Engh AM & Maduke M (2005). Cysteine accessibility in ClC-0 supports conservation of the ClC intracellular vestibule. *J Gen Physiol* **125**, 601–617.

Estévez R, Schroeder BC, Accardi A, Jentsch TJ & Pusch M (2003). Conservation of chloride channel structure revealed by an inhibitor binding site in ClC-1. *Neuron* **38**, 47–59.

Fahlke C, Rüdel R, Mitrovic N, Zhou M & George AL, Jr. (1995). An aspartic acid residue important for voltage-dependent gating of human muscle chloride channels. *Neuron* **15**, 463–472.

Fahlke C, Yu HT, Beck CL, Rhodes TH & George AL, Jr. (1997). Pore-forming segments in voltage-gated chloride channels. *Nature* **390**, 529–532.

Feng L, Campbell EB, Hsiung Y & MacKinnon R (2010). Structure of a eukaryotic CLC transporter defines an intermediate state in the transport cycle. *Science* **330**, 635–641.

Friedrich T, Breiderhoff T & Jentsch TJ (1999). Mutational analysis demonstrates that ClC-4 and ClC-5 directly mediate plasma membrane currents. *J Biol Chem* **274**, 896–902.

Günther W, Lüchow A, Cluzeaud F, Vandewalle A & Jentsch TJ (1998). ClC-5, the chloride channel mutated in Dent's disease, colocalizes with the proton pump in endocytotically active kidney cells. *Proc Natl Acad Sci U S A* **95**, 8075–8080.

Günther W, Piwon N & Jentsch TJ (2003). The ClC-5 chloride channel knock-out mouse – an animal model for Dent's disease. *Pflügers Arch* **445**, 456–462.

Hilgemann DW (1996). Unitary cardiac Na^+, Ca^{2+} exchange current magnitudes determined from channel-like noise and charge movements of ion transport. *Biophys J* **71**, 759–768.

Ishida Y, Nayak S, Mindell JA & Grabe M (2013). A model of lysosomal pH regulation. *J Gen Physiol* **141**, 705–720.

Jentsch TJ (2008). CLC chloride channels and transporters: from genes to protein structure, pathology and physiology. *Crit Rev Biochem Mol Biol* **43**, 3–36.

Leisle L, Ludwig CF, Wagner FA, Jentsch TJ & Stauber T (2011). ClC-7 is a slowly voltage-gated $2Cl^-/1H^+$-exchanger and requires Ostm1 for transport activity. *EMBO J* **30**, 2140–2152.

Lin CW & Chen TY (2003). Probing the pore of ClC-0 by substituted cysteine accessibility method using methane thiosulfonate reagents. *J Gen Physiol* **122**, 147–159.

Lippiat JD & Smith AJ (2012). The CLC-5 $2Cl^-/H^+$ exchange transporter in endosomal function and Dent's disease. *Front Physiol* **3**, 449.

Lloyd SE, Pearce SH, Fisher SE, Steinmeyer K, Schwappach B, Scheinman SJ, Harding B, Bolino A, Devoto M, Goodyer P, Rigden SP, Wrong O, Jentsch TJ, Craig IW & Thakker RV (1996). A common molecular basis for three inherited kidney stone diseases. *Nature* **379**, 445–449.

Ludewig U, Jentsch TJ & Pusch M (1997). Inward rectification in ClC-0 chloride channels caused by mutations in several protein regions. *J Gen Physiol* **110**, 165–171.

Ludwig CF, Ullrich F, Leisle L, Stauber T & Jentsch TJ (2013). Common gating of both CLC subunits underlies voltage-dependent activation of the $2Cl^-/1H^+$-exchanger ClC-7/Ostm1. *J Biol Chem* **288**, 28611–28619.

Nguitragool W & Miller C (2006). Uncoupling of a CLC Cl^-/H^+ exchange transporter by polyatomic anions. *J Mol Biol* **362**, 682–690.

Novarino G, Weinert S, Rickheit G & Jentsch TJ (2010). Endosomal chloride–proton exchange rather than chloride conductance is crucial for renal endocytosis. *Science* **328**, 1398–1401.

Orhan G, Fahlke C & Alekov AK (2011). Anion- and proton-dependent gating of ClC-4 anion/proton transporter under uncoupling conditions. *Biophys J* **100**, 1233–1241.

Picollo A, Liantonio A, Didonna MP, Elia L, Camerino DC & Pusch M (2004). Molecular determinants of differential pore blocking of kidney CLC-K chloride channels. *EMBO Rep* **5**, 584–589.

Picollo A, Malvezzi M & Accardi A (2010). Proton block of the CLC-5 Cl^-/H^+ exchanger. *J Gen Physiol* **135**, 653–659.

Picollo A & Pusch M (2005). Chloride/proton antiporter activity of mammalian CLC proteins ClC-4 and ClC-5. *Nature* **436**, 420–423.

Piwon N, Günther W, Schwake M, Bösl MR & Jentsch TJ (2000). ClC-5 Cl^- channel disruption impairs endocytosis in a mouse model for Dent's disease. *Nature* **408**, 369–373.

Pusch M, Ludewig U & Jentsch TJ (1997). Temperature dependence of fast and slow gating relaxations of ClC-0 chloride channels. *J Gen Physiol* **109**, 105–116.

Rychkov GY, Pusch M, Astill DS, Roberts ML, Jentsch TJ & Bretag AH (1996). Concentration and pH dependence of skeletal muscle chloride channel ClC-1. *J Physiol* **497**, 423–435.

Smith AJ & Lippiat JD (2010). Voltage-dependent charge movement associated with activation of the CLC-5 $2Cl^-/1H^+$ exchanger. *FASEB J* **24**, 3696–3705.

Stauber T & Jentsch TJ (2013). Chloride in vesicular trafficking and function. *Annu Rev Physiol* **75**, 453–477.

Stauber T, Weinert S & Jentsch TJ (2012). Cell biology and physiology of CLC chloride channels and transporters. *Compr Physiol* **2**, 1745–1766.

Steinmeyer K, Schwappach B, Bens M, Vandewalle A & Jentsch TJ (1995). Cloning and functional expression of rat CLC-5, a chloride channel related to kidney disease. *J Biol Chem* **270**, 31172–31177.

Traverso S, Elia L & Pusch M (2003). Gating competence of constitutively open CLC-0 mutants revealed by the interaction with a small organic inhibitor. *J Gen Physiol* **122**, 295–306.

Wang SS, Devuyst O, Courtoy PJ, Wang XT, Wang H, Wang Y, Thakker RV, Guggino S & Guggino WB (2000). Mice lacking renal chloride channel, CLC-5, are a model for Dent's disease, a nephrolithiasis disorder associated with defective receptor-mediated endocytosis. *Hum Mol Genet* **9**, 2937–2945.

Weinert S, Jabs S, Supanchart C, Schweizer M, Gimber N, Richter M, Rademann J, Stauber T, Kornak U & Jentsch TJ (2010). Lysosomal pathology and osteopetrosis upon loss of H^+-driven lysosomal Cl^- accumulation. *Science* **328**, 1401–1403.

Zdebik AA, Zifarelli G, Bergsdorf EY, Soliani P, Scheel O, Jentsch TJ & Pusch M (2008). Determinants of anion–proton coupling in mammalian endosomal CLC proteins. *J Biol Chem* **283**, 4219–4227.

Zifarelli G, De Stefano S, Zanardi I & Pusch M (2012). On the mechanism of gating charge movement of ClC-5, a human Cl^-/H^+ antiporter. *Biophys J* **102**, 2060–2069.

Zifarelli G & Pusch M (2007). CLC chloride channels and transporters: a biophysical and physiological perspective. *Rev Physiol Biochem Pharmacol* **158**, 23–76.

Zifarelli G & Pusch M (2009). Conversion of the 2 Cl^-/1 H^+ antiporter ClC-5 in a NO_3^-/H^+ antiporter by a single point mutation. *EMBO J* **28**, 175–182.

Zifarelli G & Pusch M (2010). The role of protons in fast and slow gating of the Torpedo chloride channel ClC-0. *Eur Biophys J* **39**, 869–875.

Additional information

Competing interests

None.

Author contributions

G.Z. and M.P. designed the study. G.Z. and S.D.S. performed the experiments. All authors analysed the data and wrote the manuscript. All authors read and approved the final version of the manuscript.

Funding

The financial support by the Italian Institute of Technology (progetto SEED), Telethon Italy (No. GGP12008) and Compagnia San Paolo is gratefully acknowledged.

Acknowledgements

We thank Francesca Quartino for technical assistance.